Received 3 November, 2018; | Revised <day> <Month>, <year>; | Accepted <day> <Month>, <year>

DOI: xxx/xxxx

RESEARCH ARTICLE

Robust Event-Triggered Output Feedback Learning Algorithm for Voltage Source Inverters with Unknown Load and Parameter Variations†

Kyriakos G. Vamvoudakis*[1] | Farshad R. Pour Safaei[2] | João P. Hespanha[3]

[1]Daniel Guggenheim School of Aerospace Engineering, Georgia Institute of Technology, GA 30332 USA, USA
[2]Bosch Research and Technology Center North America (RTC), Palo Alto, CA 94304, USA
[3]Department of Electrical & Computer Engineering, University of California, Santa Barbara, CA 93106, USA

Correspondence
*Kyriakos G. Vamvoudakis, Georgia Institute of Technology. Email: kyriakos@gatech.edu

Abstract

We consider the output feedback event-triggered control of an off-grid voltage source inverter (VSI) with unknown inductance - capacitance ($L - C$) filter dynamics and connected load in the presence of an input disturbance acting at the inverter. Due to uncertain dynamics and unmodeled parameters in the $L - C$ filter connected to the VSI, we use an adaptive observer to reconstruct the system's states by measuring only the voltage at the output. The control mechanism is constructed based on an impulsive actor/critic framework that approximates the cost, the event-triggered controller and the worst case disturbance and generates the desired AC output with the least energy dissipation. We provide rigorous stability proofs and illustrate the applicability of our results through a simulation example.

KEYWORDS:
VSI, output feedback, actor/critic structures, zero-sum game, event-triggered control.

1 | INTRODUCTION

Growing concerns about fossil-fuel reserves, energy security, and global warming have drawn a lot of attention to renewable energy resources[8]. The increasing use of such resources[4] with intermittent generations requires "smarter controllers" for balancing power consumption and generation, often through energy exchange. In an electrical utility grid, batteries exchange energy in the form of direct current (DC) electricity. Although there are different applications that can use DC directly, various types of applications require a VSI to convert a DC voltage to an AC voltage. VSIs are widely used for various high performance applications, such as AC motor drives, uninterruptible power supply (UPS) systems, electric vehicles, reactive power compensators and active power filters, AC power supplies and grid connected schemes[17,25].

Recently, many researchers have focused on high performance control of VSI; see[29,28] and the references therein. One of the difficulties in designing a desired optimal performance controller for a power system is the lack of a precise model. To overcome this issue, one should design high performance algorithms that are robust to parameter uncertainties and are adaptive to possible changes in the system. A natural approach to design these controllers is to take advantage of computational intelligent methods and specifically reinforcement learning methods that learn by interacting with the environment, while achieving a desired performance[21].

Different methods have been widely used in optimizing controllers and maintaining the appropriate terminal voltage, increasing real-time responsiveness to varying power loads, component failures, and improving the transient behavior of power systems

†This work was supported in part by NATO under grant No. SPS G5176, by an NSF CAREER CPS-1851588, by the Department of Energy, and by an ARO grant W911NF-09-D-0001 (Inst. for Collaborative Biotechnologies).

by using optimal neuro-adaptive controllers[6,9,24]. As stated in[31], there is an emergent need for computational intelligent controllers that allow the smart grid to self-heal, resist attacks, allow dynamic optimization of the operation, and improve power quality and efficiency. Following this line of research,[28] proposes an integral reinforcement learning algorithm to achieve the desired voltage magnitude and frequency at the load, without having full information about the dynamics of the systems. Inspired by these ideas, we design a controller for a VSI to produce a desired voltage in the presence of an input disturbance (e.g., transients, interruption, overvoltage (surge), undervoltage (sag), voltage fluctuations, electrical noise, adversary).

We further, consider a bandwidth "effective" implementation of the controller by applying the ideas of event-triggering mechanisms where the controller requests for new current and voltage measurements only when needed. This can be very effective in islanded inverters where battery lifetime is of concern. The event-triggered control algorithms[12] are composed of a feedback controller updated based on sampled state and the event triggering mechanism that determines the transmission time of the output of the controller to a Zero-Order-Hold (ZOH) actuator. Communication is a limited resource and fast sampling that is required in continuous sampled controllers is impossible in small-battery devices that run $24/7$. The authors in[22] studies the event-triggered control problem for nonlinear systems with partial state and output feedback but perform offline computation and do not have any optimality guarantees. On the contrary the work of[7] , proposes an event-triggered control framework for a class of nonlinear feedback systems that guarantees a level of performance and avoids Zeno behavior but still requires the system dynamics and requires offline computations. Our work uses reinforcement learning ideas to perform only online computations while guaranteeing a quantifiable performance.

Contributions

The contributions of the present paper are as follows. First, we combine reinforcement learning, game theory and event-triggered control in a unique framework to design an off-grid VSI to produce the desired AC voltage at the load, while attenuating input disturbances. Since in real scenarios, one can only measure the voltage at the inductance - capacitance ($L-C$) filter, we use an adaptive observer to estimate the states online, while also overcoming the need to know the system dynamics that include the values of the inductors, capacitors of the $L-C$ filter, load and parasitic resistances, which are not known exactly or change with time. Furthermore, the controller that opens and closes the switches is based on an event-triggering mechanism that updates its output only when it is about to lose optimality or stability. This is useful especially in off-grid VSIs where periodically monitoring and controlling is expensive due to shared channels and cloud-integrated information. Finally, an actor/critic mechanism based on impulsive dynamics is used to approximate the cost, the event-triggered controller, and the worst case input disturbance in real time.

Structure

The paper is structured as follows. Section II formulates the problem. A state observer is used to overcomes the need to know the system dynamics by only measuring the output voltage, and not the current, in Section III. An event-based control mechanism based on the state of the observer is provided in Section IV. Section V presents an impulsive learning algorithm to approximate the cost, the event-triggered controller, and the worst case input disturbance in real time. Simulation results are shown in Section VI. Finally Section VII concludes, and talks about future work.

2 | PROBLEM FORMULATION

Our goal is to design a controller that attenuates an input disturbance while converting *DC voltage to AC voltage* by appropriately opening and closing switches, namely a single phase off-grid VSI, with guaranteed performance, robustness, limited bandwidth and without any knowledge of the system's dynamics and load. Figure 1 shows the VSI with an $L-C$ filter that is used to reduce the switching harmonics entering the distribution network.

Before we proceed to the design of the controller, let us consider a VSI with an $L-C$ filter as shown in Figure 1, and a linear resistive load. Later, we shall see that our algorithm is independent of the load, which could be modeled by any linear or nonlinear function.

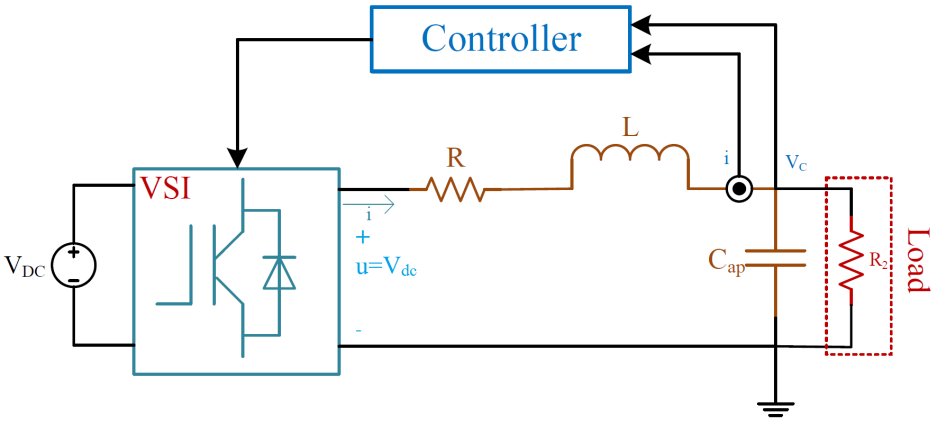

FIGURE 1 VSI filtered by an $L-C$ filter connected to a linear load.

2.1 | VSI State Space Description

The state-space representation of the system shown in Figure 1 is given by,

$$\dot{x}(t) = Ax(t) + Bu(t) + Kd(t) \equiv \begin{bmatrix} -\frac{R}{L} & -\frac{1}{L} \\ \frac{1}{C_{\text{ap}}} & -\frac{1}{C_{\text{ap}}R_2} \end{bmatrix} x + \begin{bmatrix} \frac{1}{L} \\ 0 \end{bmatrix} u + Kd,$$
$$y(t) = C^{\mathrm{T}}x(t) \equiv \begin{bmatrix} 0 & 1 \end{bmatrix} x(t),\ t \geq 0 \tag{1}$$

where $x_1 = i,\ x_2 = V_C$ are the states of the system, $u \in \mathbb{R}$ denotes the control input denoted as V_{dc} in Figure 1, $K \in \mathbb{R}^{2\times 1}$ is the disturbance matrix, and $d \in \mathbb{R}$ is the unknown input disturbance (e.g., transients, interruption, overvoltage (surge), undervoltage (sag), voltage fluctuations, electrical noise) with a known upper bound d_M. The output of this system is the voltage across the load. For simplicity, we will omit the time dependence, and write e.g., x instead of $x(t)$. In order to achieve the desired frequency ω_0, and RMS voltage V, we use the following exosystem initialized at the right amplitude:

$$\dot{Z} = A_Z Z \equiv \begin{bmatrix} 0 & \omega_0 \\ -\omega_0 & 0 \end{bmatrix} Z,\ Z(0) = \begin{bmatrix} \sqrt{2}\,V \\ 0 \end{bmatrix},$$
$$y_z = C_Z^{\mathrm{T}} Z \equiv \begin{bmatrix} 1 & 0 \end{bmatrix} Z,\ t \geq 0, \tag{2}$$

where $Z \in \mathbb{R}^2$ denotes the state of the exosystem, and $y_z \in \mathbb{R}$ its output. To save actuator resources, the controller works with a version of the state that is sampled at a monotonically increasing sequence of sampling instants $\{r_j\}_{j=0}^{\infty}$, where r_j is the j-th sampling instant with $r_{j+1} > r_j, j \in \mathbb{N}$. The output of the *sampled-data component* is a sequence of sampled states $\bar{x}_j,\ j \in \mathbb{N}$, where $\bar{x}_j = x(r_j)$ for all $t \in (r_j, r_{j+1}],\ j \in \mathbb{N}$. The controller maps the sampled states onto a control vector $\hat{u}_j,\ j \in \mathbb{N}$, which after using a zero-order hold (ZOH) becomes a piecewise continuous input signal.

2.2 | Performance Design

We shall focus our attention on designing a performance index that tracks the output of the exosystem (2), by using the least amount of energy, attenuating the disturbance with the input voltage inside the interval $[-V_{\text{dc}}, V_{\text{dc}}]$. We shall see later that this interval will be finally mapped to the discrete set $\{-V_{\text{DC}}, V_{\text{DC}}\}$. Hence, our goal is to determine the values for u, and d to minimize and maximize, respectively an infinite horizon cost functional of the following form,

$$J(x(0), (y(0) - y_z(0)); u, d) = \int_0^{\infty} \left(x^{\mathrm{T}}Qx + R_s(u) - \gamma^2 \|d\|^2 + (y - y_z)^{\mathrm{T}} Q_r (y - y_z) \right) \mathrm{d}t, \tag{3}$$

where Q, Q_r are user defined non-negative matrices of appropriate dimensions, $\gamma > \gamma^* \geq 0$, where γ^* is the smallest γ for which the criterion (3) can be made finite[30]. In order to force bounded inputs ($|u| \leq V_{\text{dc}}$) one should use $R_s(u) = 2\int_0^u (\theta^{-1}(v))^{\mathrm{T}} dv := 2\int_0^u (V_{\text{dc}} \tanh^{-1}(\frac{v}{V_{\text{dc}}}))^{\mathrm{T}} dv,\ \forall u$ used to map $\mathbb{R}$ onto the interval $(-V_{\text{dc}}, V_{\text{dc}})$. The term $x^{\mathrm{T}}Qx$ penalizes the current, and the voltage

to encourage a smooth transient response, whereas the term $(y-y_z)^{\mathrm{T}}Q_r(y-y_z)$ favors good tracking of the exosystem. Inspired by the work on implicit model following in [1], we shall use an augmented system $x_{\text{aug}} := \begin{bmatrix} x \\ Z \end{bmatrix} \in \mathbb{R}^4$ that augments the state of the system (1) with the state of the exosystem (2). The dynamics of the augmented states are given by,

$$\dot{x}_{\text{aug}} = \begin{bmatrix} A & 0_{2\times 2} \\ 0_{2\times 2} & A_Z \end{bmatrix} x_{\text{aug}} + \begin{bmatrix} \frac{1}{L} \\ \mathbf{0}_3 \end{bmatrix} u + \begin{bmatrix} K \\ \mathbf{0}_2 \end{bmatrix} d,\ t \geq 0. \tag{4}$$

Following [1], we minimize the conflict between the need to minimize the tracking error $(y-y_z)^{\mathrm{T}}Q_r(y-y_z)$, and to keep $x^{\mathrm{T}}Qx$ small, by adjusting (3) as follows:

$$J(x_{\text{aug}}(0); u, d) = \int_0^\infty \left(R_s(u) - \gamma^2 \|d\|^2 + x_{\text{aug}}^{\mathrm{T}}\tilde{Q}x_{\text{aug}}\right)\mathrm{d}t := \int_0^\infty c(x_{\text{aug}}, u, d)\mathrm{d}t, \tag{5}$$

where,

$$\tilde{Q} := \begin{bmatrix} \tilde{Q}_{11} & \tilde{Q}_{12} \\ \tilde{Q}_{21} & \tilde{Q}_{22} \end{bmatrix} \tag{6}$$

with $\tilde{Q}_{11} := C_r^{\mathrm{T}}QC_r + CQ_rC^{\mathrm{T}}$, $C_r := [I - C(C^{\mathrm{T}}C)^{-1}C^{\mathrm{T}}]$, $\tilde{Q}_{12} := -(C_r^{\mathrm{T}}QC_r + CQ_rC^{\mathrm{T}})C(C^{\mathrm{T}}C)^{-1}C_Z^{\mathrm{T}}$, $\tilde{Q}_{21} := -C_Z(C^{\mathrm{T}}C)^{-1}C^{\mathrm{T}}(C_r^{\mathrm{T}}QC_r + CQ_rC^{\mathrm{T}})$, $\tilde{Q}_{22} := C_Z(C^{\mathrm{T}}C)^{-1}C^{\mathrm{T}}(C_r^{\mathrm{T}}QC_r + CQ_rC^{\mathrm{T}})C(C^{\mathrm{T}}C)^{-1}C_Z^{\mathrm{T}}$. We are interested in finding a Nash equilibrium policy (saddle point) $u^*,\ d^*$ [2] that satisfies,

$$J(\cdot; u^*, d) \leq J(\cdot; u^*, d^*) \leq J(\cdot; u, d^*),\ \forall u, d, \tag{7}$$

where for simplicity, we have omitted the dependence on the initial conditions.

3 | ADAPTIVE OBSERVER

Since the parasitic quantities in the $L-C$ filter can vary or are not known exactly, we cannot construct the controller directly by using full-state feedback, i.e., measuring the current, and the voltage. To overcome this difficulty, a state observer based on the work of [15,18] is employed to overcome the knowledge of the system dynamics by measuring only the output voltage. No output-matching or growth-rate conditions are required in such approach.

Since in our observer design, we consider unknown dynamics, we rewrite (1) in a more general form as,

$$\begin{aligned} \dot{x} &= A_O x + \mathrm{F}(x) + \mathrm{G}u + Kd, \\ y &= C^{\mathrm{T}}x, \end{aligned} \tag{8}$$

where $A_O \in \mathbb{R}^{2\times 2}$ is a known matrix such that the pair (A_O, C) is in an observable canonical form as given in [18], but the functions $F(x) := Ax$, and $\mathrm{G} := B$ will be considered to be unknown. By using universal approximation properties [14], we know that, for a given compact set $\Omega \subseteq \mathbb{R}^2$, there exists a sufficiently large number of basis functions N such that,

$$\mathrm{F}(x) = W_1^{\mathrm{T}}\Phi(x) + \epsilon_1(x),\ \forall x, \tag{9}$$

where $W_1 \in \mathbb{R}^{N\times 2}$ are the ideal weights bounded by a constant over the compact set Ω as $\|W_1\| \leq W_{1\max}$, $\Phi(x)$ is the basis function bounded above by a constant Φ_M, and $\epsilon_1(x) \in \mathbb{R}^2$ is the reconstruction error bounded above in the compact set Ω by $\epsilon_{1\max}$. We can do similarly for the unknown function G to write,

$$\mathrm{G} = W_2^{\mathrm{T}}\Phi(x) + \epsilon_2(x),\ \forall x, \tag{10}$$

where $W_2 \in \mathbb{R}^{N\times 2}$ are the ideal weights bounded by a constant over the compact set Ω as $\|W_2\| \leq W_{2\max}$, and $\epsilon_2(x) \in \mathbb{R}^2$ is the reconstruction error bounded above in the compact set Ω by $\epsilon_{2\max}$.

Let $\hat{W}_1,\ \hat{W}_2$ denote the estimates of the ideal weights W_1, and W_2, respectively. Defining the weight estimation errors as, $\tilde{W}_i := W_i - \hat{W}_i,\ i = \{1, 2\}$ and by noting that the basis functions are bounded, this means that $(\Phi(x) - \Phi(\hat{x}))$ is bounded above by $\tilde{\Phi}_M$.

Using the approximations of (9), and (10), a state estimator for (8) can be expressed as, $\dot{\hat{x}} = A_O\hat{x} + P^{-1}C\left(\hat{W}_1^{\mathrm{T}}\Phi(\hat{x}) + \hat{W}_2^{\mathrm{T}}\Phi(\hat{x})u\right) + L_O(y - C^{\mathrm{T}}\hat{x})$, $\hat{y} = C^{\mathrm{T}}\hat{x}$, where y denotes the measured output, the observer gain $L_O \in \mathbb{R}^2$ is chosen such that $A_{\mathrm{OC}} := A_O - L_O C$ is Hurwitz, and $P \succ 0$ such that, $A_{\mathrm{OC}}^{\mathrm{T}}P + PA_{\mathrm{OC}} = -qI_2$ with $q \in \mathbb{R}^+$ being a design parameter and $I_2 := \begin{bmatrix}1 & 0\\ 0 & 1\end{bmatrix}$. We will define the state, and output errors as, $\tilde{x} := x - \hat{x}$, and $\tilde{y} := y - \hat{y}$, respectively. We now can write the error state dynamics as, $\dot{\tilde{x}} = A_{\mathrm{OC}}\tilde{x} + P^{-1}C\left(\tilde{W}_1^{\mathrm{T}}\Phi(\hat{x}) + W_1^{\mathrm{T}}(\Phi(x) - \Phi(\hat{x})) + \epsilon_1(x) + \left(\tilde{W}_2^{\mathrm{T}}\Phi(\hat{x}) + W_2^{\mathrm{T}}(\Phi(x) - \Phi(\hat{x})) + \epsilon_2(x)\right)u\right)$, $\tilde{y} = C^{\mathrm{T}}\tilde{x}$.

Remark 1. Note that in a real implementation, the current will not be available for direct measurement, but only the output voltage, and hence an output feedback approach will be more appealing.

Remark 2. Note that the observer design is obtained without requiring any strictly positive real condition with the use of the term $P^{-1}C$ as proved in [15].

The following theorem shows how to tune the weights $\hat{W}_1$, and $\hat{W}_2$ to drive the estimation errors $\tilde{x}$, $\tilde{y}$ to zero.

Theorem 1. Suppose that the control input $u(t)$ is upper bounded by u_M, and that the state remains inside the compact set Ω. Consider the observer in (8) with, $\dot{\hat{W}}_1 = -\alpha_1 B_1\hat{W}_1 + (y - \hat{y})B_1\Phi(\hat{x})$, and $\dot{\hat{W}}_2 = -\alpha_2 B_2\hat{W}_2 + (y - \hat{y})B_2\Phi(\hat{x})u$ where α_1, $\alpha_2 \in \mathbb{R}^+$ and positive definite symmetric matrices B_1, B_2. Then the state error $\tilde{x}$ and the weight estimation errors $\tilde{W}_1$, and $\tilde{W}_2$ are uniformly ultimately bounded (UUB).

Proof. The proof is similar to [15] (see Theorem 1) and [18] (see Theorem 3.1). □

Now the augmented system dynamics from (4) are given by,

$$\dot{\hat{x}}_{\mathrm{aug}} = \tilde{f}(\hat{x}_{\mathrm{aug}}) + \tilde{g}u + \begin{bmatrix}K\\ \mathbf{0}_2\end{bmatrix}d, \tag{11}$$

where $\hat{x}_{\mathrm{aug}} := \begin{bmatrix}\hat{x}\\ Z\end{bmatrix} \in \mathbb{R}^4$, is the estimated augmented state, $\tilde{f}(\hat{x}_{\mathrm{aug}}) := \begin{bmatrix}A_O\hat{x} + P^{-1}C\hat{W}_1^{\mathrm{T}}\Phi(\hat{x}) + L_O(y - C^{\mathrm{T}}\hat{x})\\ A_Z\end{bmatrix}$ and $\tilde{g} := \begin{bmatrix}P^{-1}C\hat{W}_2^{\mathrm{T}}\Phi(\hat{x})\\ \mathbf{0}_2\end{bmatrix}$.

Remark 3. Note that since the learning framework is developed for (11) and not for (1), as stated earlier we will be able to be independent of the load, which could be modeled by any linear or nonlinear function.

4 | EVENT-TRIGGERED ZERO-SUM GAME DESIGN

Our next step is to design an event-based control mechanism based on the state of the observer defined in the previous section, which is now fully available for feedback.

The ultimate goal is to compute the cost function V^* defined $\forall t \geq 0$ by,

$$V^*(\hat{x}_{\mathrm{aug}}(t)) := \min_u \max_d \int_t^\infty c(\hat{x}_{\mathrm{aug}}, u, d)\mathrm{d}\tau, \tag{12}$$

subject to the system dynamics constraint (4) and given bounded inputs inside the interval $[-V_{\mathrm{dc}}, V_{\mathrm{dc}}]$.

The controller works with a sampled version of the state and is updated only when an event is triggered. In other words, we have

$$\bar{x}_{\mathrm{aug}}(t) = \begin{cases}\hat{x}_{\mathrm{aug}}(r_j), & t = r_j\\ \bar{x}_{\mathrm{aug}}(t), & \forall t \in (r_j, r_{j+1}].\end{cases}$$

We define the gap between the sampled version of the state and the actual state as, $e(t) := \bar{x}_{\text{aug}}(t) - \hat{x}_{\text{aug}}(t)$. We shall see that when a condition is violated, or about to be violated a new event will be triggered to force the gap to zero, i.e.

$$e(t) = \begin{cases} 0, & t = r_j \\ \bar{x}_{\text{aug}}(t) - \hat{x}_{\text{aug}}(t), & \forall t \in (r_j, r_{j+1}]. \end{cases}$$

We can derive the Hamiltonian associated with the system (11) as follows,

$$H(\hat{x}_{\text{aug}}, u, d, \frac{\partial V^*(\hat{x}_{\text{aug}})}{\partial \hat{x}_{\text{aug}}}) = \frac{\partial V^*(\hat{x}_{\text{aug}})}{\partial \hat{x}_{\text{aug}}}^{\text{T}} \left(\tilde{f}(\hat{x}_{\text{aug}}) + \tilde{g}u + \begin{bmatrix} K \\ \mathbf{0}_2 \end{bmatrix} d \right) + c(\hat{x}_{\text{aug}}, u, d), \forall \hat{x}_{\text{aug}}, u, d. \tag{13}$$

We need to find the control input and the disturbance such that the performance (12) is minimized with respect to the control and maximized with respect to the disturbance. For the optimal control input we have,

$$u^*(\hat{x}_{\text{aug}}) = -\theta\{\frac{1}{2}\tilde{g}^{\text{T}} \frac{\partial V^*(\hat{x}_{\text{aug}})}{\partial \hat{x}_{\text{aug}}}\} \tag{14}$$

and since we have event-triggering controllers, we shall write (14) as

$$u^*(\bar{x}_{\text{aug}}) = -\theta\{\frac{1}{2}\tilde{g}(\bar{x}_{\text{aug}})^{\text{T}} \frac{\partial V^*(\bar{x}_{\text{aug}})}{\partial \hat{x}_{\text{aug}}}\}, \text{ for } t \in (r_j, r_{j+1}] \text{ and } j \in \mathbb{N}, \tag{15}$$

and for the disturbance (where the controller holds a copy of it) we get

$$d^*(\hat{x}_{\text{aug}}) = \frac{1}{2\gamma^2} \begin{bmatrix} K \\ \mathbf{0}_2 \end{bmatrix}^{\text{T}} \frac{\partial V^*(\hat{x}_{\text{aug}})}{\partial \hat{x}_{\text{aug}}}, \forall t \geq 0. \tag{16}$$

Substituting (14) and (16) into (13), we get a Hamilton-Jacobi-Isaacs (HJI) equation with continuous control updates, $\forall \hat{x}_{\text{aug}}$ of the following form,

$$H(\hat{x}_{\text{aug}}, u^*(\hat{x}_{\text{aug}}), d^*(\hat{x}_{\text{aug}}), \frac{\partial V^*(\hat{x}_{\text{aug}})}{\partial \hat{x}_{\text{aug}}}) = 0, \tag{17}$$

and after substituting (15) and (16) into (13) we get a Hamilton-Jacobi-Isaacs (HJI) equation with event-triggered control updates, $\forall \hat{x}_{\text{aug}}, \bar{x}_{\text{aug}}$ of the following form,

$$H(\hat{x}_{\text{aug}}, u^*(\bar{x}_{\text{aug}}), d^*(\hat{x}_{\text{aug}}), \frac{\partial V^*(\hat{x}_{\text{aug}})}{\partial \hat{x}_{\text{aug}}}) = \frac{\partial V^*(\hat{x}_{\text{aug}})}{\partial \hat{x}_{\text{aug}}}^{\text{T}} \left(\tilde{f}(\hat{x}_{\text{aug}}) + \tilde{g}u^*(\bar{x}_{\text{aug}}) + \begin{bmatrix} K \\ \mathbf{0}_2 \end{bmatrix} d^*(\hat{x}_{\text{aug}}) \right) + c(\hat{x}_{\text{aug}}, u^*(\bar{x}_{\text{aug}}), d^*(\hat{x}_{\text{aug}})), \tag{18}$$

which are eventually the equations we would like to solve.

The following assumptions are classical in event-triggered control[26] and are needed before one can proceed to the design of the triggering condition, the existence of solution and stability theorem for the event-triggered scheme. Specifically the following Lipschitz assumption on the controller is a standard assumption in event-triggered control,[3,10,23,26,27], and is satisfied in many applications (e.g. when the controller is affine with respect to the gap signal) as was also mentioned in[20]. By changing such constant, we will be controlling the asynchronous occurrence of communication events through the threshold-based scheme in a way that may drastically reduce the number of such events while still guaranteeing convergence, stability and a quantified optimality.

Assumption 1. The controller is locally Lipschitz continuous $\forall \hat{x}_{\text{aug}},\ \bar{x}_{\text{aug}}$, $\left\| u(\hat{x}_{\text{aug}}) - u(\bar{x}_{\text{aug}}) \right\| = \left\| u(\hat{x}_{\text{aug}}) - u(\hat{x}_{\text{aug}} + e) \right\| \leq L_D \|e\|$, where L_D is a non-negative real Lipschitz constant.

Assumption 2. The closed-loop system is locally Lipschitz continuous with respect to the state $\hat{x}_{\text{aug}}$ and to the gap e.

Lemma 1. Suppose that Assumptions 1, 2 hold. Then the gap between the HJI with the continuous-sampled controller given by (17) and the HJI with the event-triggered controller given by (18) is,

$$H(\hat{x}_{\text{aug}}, u^*(\bar{x}_{\text{aug}}), d^*(\hat{x}_{\text{aug}}), \frac{\partial V^*(\hat{x}_{\text{aug}})}{\partial \hat{x}_{\text{aug}}}) = R_s\left(u^*(\hat{x}_{\text{aug}}) - u^*(\bar{x}_{\text{aug}})\right),\ \forall \bar{x}_{\text{aug}}, \hat{x}_{\text{aug}}, \tag{19}$$

where $R_s\left(u^*(\hat{x}_{\text{aug}}) - u^*(\bar{x}_{\text{aug}})\right) = 2\int_0^{\left(u^*(\hat{x}_{\text{aug}}) - u^*(\bar{x}_{\text{aug}})\right)} (\theta^{-1}(v))^{\text{T}} dv, \forall u^*(\hat{x}_{\text{aug}}), u^*(\bar{x}_{\text{aug}})$.

Proof. The required result can be proved by taking the difference between (17) and (18) and completing the squares. □

Remark 4. For nonlinear systems, there is no clear derivation for L_D, and picking the Lipschitz constant is dependent on the application and the available resources.

The result of Lemma 1 motivates the selection of the triggering instants r_j based on a triggering rule that will be defined in the following Theorem. A scheme of the event-triggered controller is shown in Figure 2.

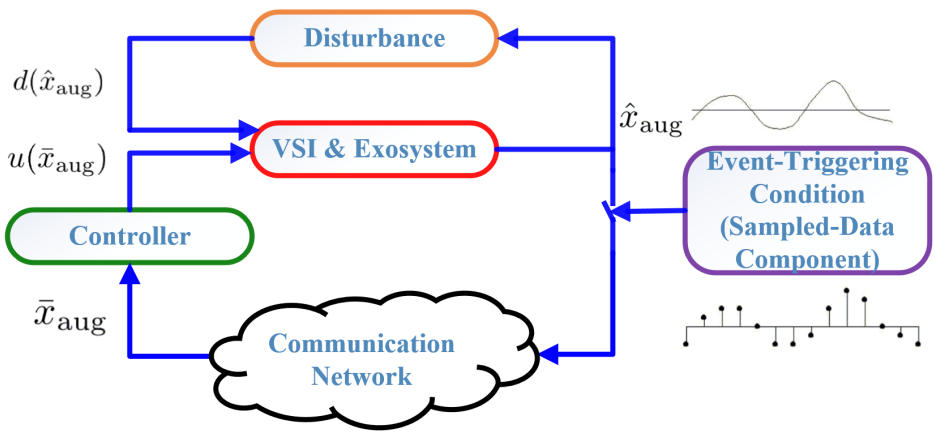

FIGURE 2 The scheme of the sampled-data control system.

The formulation of the HJI equation (17) with $\tilde{Q}$ picked as in (6) to achieve tracking works only for finite horizon optimization. The problem is that (5) will have an infinite value and so that the optimization (12) is not well defined. Moreover the HJI (17) requires full knowledge of the dynamics of each VSI which in real world problems will limit the application of the developed algorithm because of unknown quantities and unmodeled dynamics. From[32], we know that an equivalent formulation of the (17) that does not involve the dynamics and produces a finite cost is given as,

$$V(\hat{x}_{\text{aug}}(t-T)) = \int_{t-T}^{\mathrm{T}} \left(R_s(u^*) - \gamma^2 \|d^*\|^2 + \hat{x}_{\text{aug}}^{\mathrm{T}} \tilde{Q} \hat{x}_{\text{aug}}\right) \mathrm{d}\tau + V(\hat{x}_{\text{aug}}(t)),$$

for any time $t \geq 0$ and time interval $T > 0$.

Theorem 2. Suppose that Assumptions 1-2 and Lemma 1 hold, and that there exists a continuously differentiable, positive definite function V that satisfies the following HJI inequality $\forall \hat{x}_{\text{aug}}$ given (11),

$$\int_{t-T}^{t} \left(\dot{V}(\hat{x}_{\text{aug}}) + R_s(u^*) - \gamma^2 \|d^*\|^2 + \hat{x}_{\text{aug}}^{\mathrm{T}} \tilde{Q} \hat{x}_{\text{aug}}\right) \mathrm{d}\tau \leq 0, \forall t, \ \forall \hat{x}_{\text{aug}}, \tag{20}$$

with $V(0) = 0$ and a constant $\gamma \in \mathbb{R}^+$. The closed-loop system with event-triggered control policy given by,

$$u(\bar{x}_{\text{aug}}) = u^*(\bar{x}_{\text{aug}}) := -\theta\{\frac{1}{2}\tilde{g}(\bar{x}_{\text{aug}})^{\mathrm{T}} \frac{\partial V(\bar{x}_{\text{aug}})}{\partial \hat{x}_{\text{aug}}}\} \tag{21}$$

for $t \in (r_j, r_{j+1}]$ and all $j \in \mathbb{N}$ and disturbance given by

$$d(\hat{x}_{\text{aug}}) = d^*(\hat{x}_{\text{aug}}) := \frac{1}{2\gamma^2} \begin{bmatrix} K \\ \mathbf{0}_2 \end{bmatrix}^{\mathrm{T}} \frac{\partial V(\hat{x}_{\text{aug}})}{\partial \hat{x}_{\text{aug}}} \tag{22}$$

is asymptotically-stable given that the following triggering condition holds $\forall t \geq 0$,

$$R_s(L_D \|e\|) \leq (1-\beta^2)\underline{\lambda}(\tilde{Q}) \left\|\hat{x}_{\text{aug}}\right\|^2 + R_s(u(\bar{x}_{\text{aug}})), \tag{23}$$

for some user defined $\beta \in [0,1]$. Moreover, the control (21) and (22) lead to a cost of, $J^*(\cdot; u^*, d^*) = V^*(\hat{x}_{\text{aug}}(0)) + \int_0^\infty R_s\left(u^*(\hat{x}_{\text{aug}}) - u^*(\bar{x}_{\text{aug}})\right) \mathrm{d}t$.

Proof. The proof is provided in the appendix. □

Remark 5. It is worth noting that if one needs to approach the performance of the continuous sampled controller we need to make the term $R_s\left(u^*(\hat{x}_{\text{aug}}) - u^*(\bar{x}_{\text{aug}})\right)$ as close to zero as possible by adjusting the parameter β of the triggering condition given in (23). This means that when β is close to 1 one samples more frequently whereas when β is close to zero, the inter-sampling periods become longer and the performance will be far from the continuous sampled optimal controller.

Remark 6. The techniques used in the derivation of (23) rely on Lipschitz continuity and is necessarily conservative for general nonlinear systems. It bounds the minimum inter-transmission delay as a function of the open-loop system's Lipschitz constant.

5 | LEARNING ALGORITHM

Since solving the HJI equation (17) is infeasible, we use ideas from reinforcement learning[32] and specifically an actor/critic network structure. The critic network will approximate the value function V^* in a compact set $\Omega \subseteq \mathbb{R}^4$ and the actor networks will approximate the event-triggered controller (15), and the worst case disturbance (16) as follows,

$$V^*(\hat{x}_{\text{aug}}) = W_c^* \phi_c(\hat{x}_{\text{aug}}) + \epsilon_c(\hat{x}_{\text{aug}}),\ \forall \hat{x}_{\text{aug}}, \tag{24}$$

$$u^*(\bar{x}_{\text{aug}}) = W_u^{*\mathrm{T}} \phi_u(\bar{x}_{\text{aug}}) + \epsilon_u(\bar{x}_{\text{aug}}), \forall \bar{x}_{\text{aug}}, t \in (r_j, r_{j+1}],\ j \in \mathbb{N} \tag{25}$$

$$d^*(\hat{x}_{\text{aug}}) = W_d^{*\mathrm{T}} \phi_d(\hat{x}_{\text{aug}}) + \epsilon_d(\hat{x}_{\text{aug}}),\ \forall \hat{x}_{\text{aug}}, \tag{26}$$

where the ideal weights are denoted by $W_c^* \in \mathbb{R}^{h_1}, W_u^* \in \mathbb{R}^{h_2}, W_d^* \in \mathbb{R}^{h_3}$ which are bounded as $\|W_c^*\| \leq W_{\text{cmax}}, \|W_u^*\| \leq W_{\text{umax}}, \left\|W_d^*\right\| \leq W_{\text{dmax}}$ respectively. The basis functions for the critic ϕ_c are picked in a way that as $h_1 \to \infty$, V^* is uniformly approximated and the basis functions are bounded and continuously differentiable (i.e. $\|\phi_c\| \leq \phi_{\text{cmax}}$ and $\left\|\frac{\partial \phi_c}{\partial \hat{x}_{\text{aug}}}\right\| \leq \phi_{\text{cdmax}}$). The residual error ϵ_c for (24) is assumed to satisfy $\sup_{\hat{x}_{\text{aug}} \in \Omega} \|\epsilon_c\| \leq \epsilon_{\text{cmax}}$ and $\sup_{\hat{x}_{\text{aug}} \in \Omega} \left\|\frac{\partial \epsilon_c}{\partial \hat{x}_{\text{aug}}}\right\| \leq \epsilon_{\text{cdmax}}$. Similarly for the two actors (25)-(26) the basis functions (picked so that as $h_2 \to \infty, h_3 \to \infty$ the optimal control and worst case disturbance are uniformly approximated) and residual errors are assumed to be upper bounded as $\sup_{\bar{x}_{\text{aug}} \in \Omega} \|\epsilon_u\| \leq \epsilon_{\text{umax}}$, $\|\phi_u\| \leq \phi_{\text{umax}}$, and respectively $\sup_{\hat{x}_{\text{aug}} \in \Omega} \|\epsilon_d\| \leq \epsilon_{\text{dmax}}$, $\|\phi_d\| \leq \phi_{\text{dmax}}$.

5.1 | Actor/Critic Structure

Since the ideal weights for the three approximators (24), (25) and (26), are not available, we use weight estimates for their representation and then tune them appropriately,

$$\hat{V}(\hat{x}_{\text{aug}}) = \hat{W}_c \phi_c(\hat{x}_{\text{aug}}),\ \forall \hat{x}_{\text{aug}}, \tag{27}$$

$$\hat{u}(\bar{x}_{\text{aug}}) = \hat{W}_u^{\mathrm{T}} \phi_u(\bar{x}_{\text{aug}}),\ \forall \bar{x}_{\text{aug}}, t \in (r_j, r_{j+1}],\ j \in \mathbb{N} \tag{28}$$

$$\hat{d}(\hat{x}_{\text{aug}}) = \hat{W}_d^{\mathrm{T}} \phi_d(\hat{x}_{\text{aug}}),\ \forall \hat{x}_{\text{aug}}. \tag{29}$$

Now we shall follow techniques from adaptive control[16] to design tuning laws for the aforementioned approximators.

In order to find the tuning laws for the critic we define the following error signal $e_c \in \mathbb{R}$ that is desired to be driven to zero, $e_c = \hat{W}_c^{\mathrm{T}} \Delta\phi - \hat{\pi}$, where $\Delta\phi = \phi(\hat{x}_{\text{aug}}(t)) - \phi(\hat{x}_{\text{aug}}(t-T))$ and $\hat{\pi} = \int_{t-T}^{\mathrm{T}} \left(R_s(\hat{u}) - \gamma^2 \left\|\hat{d}\right\|^2 + \hat{x}_{\text{aug}}^{\mathrm{T}} \tilde{Q} \hat{x}_{\text{aug}}\right) \mathrm{d}\tau$. Similarly, to find the tuning laws for the two actors we use the following error signals $e_u, e_d \in \mathbb{R}$, $e_u = \hat{W}_u^{\mathrm{T}} \phi_u(\bar{x}_{\text{aug}}) + \theta\{\frac{1}{2}\tilde{g}(\bar{x}_{\text{aug}})^{\mathrm{T}} \frac{\partial \phi_u}{\partial \hat{x}_{\text{aug}}} \hat{W}_c\}$, $e_d = \hat{W}_d^{\mathrm{T}} \phi_d(\hat{x}_{\text{aug}}) - \frac{1}{2\gamma^2} \begin{bmatrix} K \\ \mathbf{0}_2 \end{bmatrix}^{\mathrm{T}} \frac{\partial \phi_d}{\partial \hat{x}_{\text{aug}}} \hat{W}_c$.

The tuning laws for the critic and the two actors are obtained using gradient descent to drive the errors e_c, e_u, e_d to zero,

$$\dot{\hat{W}}_c = -\alpha_c \frac{\Delta\phi}{(\|\Delta\phi\|^2 + 1)^2} \left(\Delta\phi^{\mathrm{T}} \hat{W}_c + \hat{\pi}\right),\ \forall t \geq 0 \tag{30}$$

$$\dot{\hat{W}}_u = 0, \text{ for } r_j < t \leq r_{j+1}, j \in \mathbb{N}, \tag{31}$$

$$\hat{W}_u^+ = \hat{W}_u(t) - \alpha_u \phi_u(\hat{x}_{\text{aug}}(t))\left(\hat{W}_u^{\text{T}}\phi_u(\hat{x}_{\text{aug}}(t))\theta\{\frac{1}{2}\tilde{g}(\hat{x}_{\text{aug}}(t))^{\text{T}}\frac{\partial \phi_c}{\partial \hat{x}_{\text{aug}}}\hat{W}_c\}\right)^{\text{T}}, \text{ for } t = r_j,\ j \in \mathbb{N}, \tag{32}$$

and $\forall t \geq 0$

$$\dot{\hat{W}}_d = -\alpha_d \phi_d(\hat{x}_{\text{aug}})\left(\hat{W}_d^{\text{T}}\phi_d(\hat{x}_{\text{aug}}) - \frac{1}{2\gamma^2}\begin{bmatrix} K \\ \mathbf{0}_2 \end{bmatrix}^{\text{T}} \frac{\partial \phi_c}{\partial \hat{x}_{\text{aug}}}\hat{W}_c\right)^{\text{T}}. \tag{33}$$

Since the control $u = V_{\text{dc}}$ is obtained by connecting V_{dc} in Figure 1 to either $+V_{\text{DC}}$ or $-V_{\text{DC}}$ we must have $u \in \{-V_{\text{DC}}, +V_{\text{DC}}\}$, and for that reason one should pass the control input through a hard limiter that limits its output to $\pm V_{\text{DC}}$, i.e., $\hat{u}_{\text{dc}} = V_{\text{DC}}\ \theta_{\text{hlim}}(\hat{u})$; $\theta_{\text{hlim}}(\hat{u}) = \begin{cases} -1, & \hat{u} < 0 \\ 1, & \hat{u} \geq 0. \end{cases}$

We shall define the following notations for the weight estimation errors, $\tilde{W}_c := W_c^* - \hat{W}_c$, $\tilde{W}_u := W_u^* - \hat{W}_u$ and $\tilde{W}_d := W_d^* - \hat{W}_d$. The weight estimation error dynamics are given for the critic as,

$$\dot{\tilde{W}}_c = -\alpha_c \frac{\Delta\phi\Delta\phi^{\text{T}}}{(\|\Delta\phi\|^2 + 1)^2}\tilde{W}_c + \alpha_c \frac{\Delta\phi}{(\|\Delta\phi\|^2 + 1)^2}\epsilon_{\tilde{W}_c}, \forall t \geq 0. \tag{34}$$

The weight estimation error dynamics for the controller actor are given as, $\dot{\tilde{W}}_u = 0$, for $r_j < t \leq r_{j+1}$, $j \in \mathbb{N}$, and, $\tilde{W}_u^+ = \tilde{W}_u(t) - \alpha_u \phi_u(\hat{x}_{\text{aug}}(t))\left(\tilde{W}_u^{\text{T}}\phi_u(\hat{x}_{\text{aug}}(t)) + \epsilon_u^{\text{T}}\phi_u(\hat{x}_{\text{aug}}(t)) + \theta\{\frac{1}{2}\tilde{g}(\hat{x}_{\text{aug}}(t))^{\text{T}}\frac{\partial \phi_u}{\partial \hat{x}_{\text{aug}}}\tilde{W}_c\} + \theta\{\frac{1}{2}\tilde{g}(\hat{x}_{\text{aug}}(t))^{\text{T}}\frac{\partial \epsilon_c}{\partial \hat{x}_{\text{aug}}}\}\right)^{\text{T}}$, for $t = r_j, j \in \mathbb{N}$, and finally for the disturbance actor as,

$$\dot{\tilde{W}}_d = -\alpha_d \phi_d(\hat{x}_{\text{aug}})\left(\tilde{W}_d^{\text{T}}\phi_d(\hat{x}_{\text{aug}}) + \epsilon_d^{\text{T}}\phi_d(\hat{x}_{\text{aug}}) - \frac{1}{2\gamma^2}\begin{bmatrix} K \\ \mathbf{0}_2 \end{bmatrix}^{\text{T}} \frac{\partial \phi_c}{\partial \hat{x}_{\text{aug}}}\tilde{W}_c - \frac{1}{2}\begin{bmatrix} K \\ \mathbf{0}_2 \end{bmatrix}^{\text{T}} \frac{\partial \epsilon_c}{\partial \hat{x}_{\text{aug}}}\right)^{\text{T}}, \forall t \geq 0, \tag{35}$$

where $\epsilon_{\tilde{W}_c} = -\frac{\partial \epsilon_c}{\partial \hat{x}_{\text{aug}}}\left(\tilde{f}(\hat{x}_{\text{aug}}) + \tilde{g}\hat{u}(\bar{x}_{\text{aug}}) + \begin{bmatrix} K \\ \mathbf{0}_2 \end{bmatrix}\hat{d}(\hat{x}_{\text{aug}})\right)$. The following main theorem is proved in the next subsection and states that the impulsive closed-loop is UUB [11, 19].

Theorem 3. Suppose that Assumptions 1,2 hold and that the signal $\Delta := \frac{\Delta\phi}{\|\Delta\phi\|^2+1}$ is persistently exciting over the interval $[t, t + T_{\text{PE}}]$ with $T_{\text{PE}} \in \mathbb{R}^+$ and $\int_t^{t+T_{\text{PE}}} \Delta\Delta^{\text{T}} d\tau \geq \mu I$ with $\mu \in \mathbb{R}^+$ and I an identity matrix of appropriate dimensions. Consider the system dynamics given by (11), the critic approximator given by (27), the event-triggered control given by (28) and the worst case disturbance given by (29). The tuning law for the weights of of the critic is given by (30), the tuning law for the actor weights are given by the impulsive system (31)-(32) for the event-triggered controller and by (33) for the disturbance. Then the equilibrium point of the impulsive system $\psi := \begin{bmatrix} \hat{x}_{\text{aug}}^{\text{T}} & \bar{x}_{\text{aug}}^{\text{T}} & \tilde{W}_c^{\text{T}} & \tilde{W}_u^{\text{T}} & \tilde{W}_d^{\text{T}} \end{bmatrix}^{\text{T}}$ for all initial conditions $\psi(0)$ in the compact set is UUB given that the following condition holds $\forall t \geq 0$,

$$R_s(L_D\|e\|) \leq (1 - \beta^2)\underline{\lambda}(\tilde{Q})\left\|\hat{x}_{\text{aug}}\right\|^2 + R_s(\hat{W}_u^{\text{T}}\phi_u(\bar{x}_{\text{aug}})), \forall t \geq 0, \tag{36}$$

and the following inequalities,

$$\alpha_c \underline{\lambda}\left(\frac{\Delta\phi\Delta\phi^{\text{T}}}{(\|\Delta\phi\|^2 + 1)^2}\right) - \frac{1}{2\alpha_c} > \frac{\phi_{\text{cdmax}}^2}{4\gamma^2}, \tag{37}$$

$$\phi_{\text{dmax}} > \sqrt{\frac{3}{4(1 - \frac{1}{4\gamma^2})}};\ \gamma > \frac{1}{2}, \tag{38}$$

$$0 < \alpha_u < 2, \tag{39}$$

hold.

Proof. The proof is provided in the appendix. □

Corollary 1. Suppose that the hypotheses and the statements of theorem 3 hold. Then, the policies $\hat{u}$ given by (28) and $\hat{d}$ given by (29) form an approximate Nash equilibrium (saddle point).

Proof. Follows from theorem 3. □

Remark 7. In our algorithm there are no offline computations, neither requirements for storage of any data in the memory, but everything happens as in a plug-n-play framework. The involved computation is as in many adaptive control algorithms and is dominated by the training algorithm for the adaptive observer $\hat{W}_1$ and $\hat{W}_2$ and for the actor/critic algorithm $\hat{W}_c, \hat{W}_u$ and $\hat{W}_d$ in order to approximate (27), (28), and (29) respectively. The complexity of the scheme increases with the number of basis N, h_1 and h_2. Thus, the complexity is $\mathcal{O}\big(4(N + h_1 + h_2)\big)$. It has been shown in[32] (cf. Chapter 7) and[16] that the convergence rate of gradient descent algorithms of the form (30), (32) and (33) converge exponentially fast with rate that depends on the level of excitation μ and the tuning gains $\alpha_c, \alpha_u, \alpha_d$.

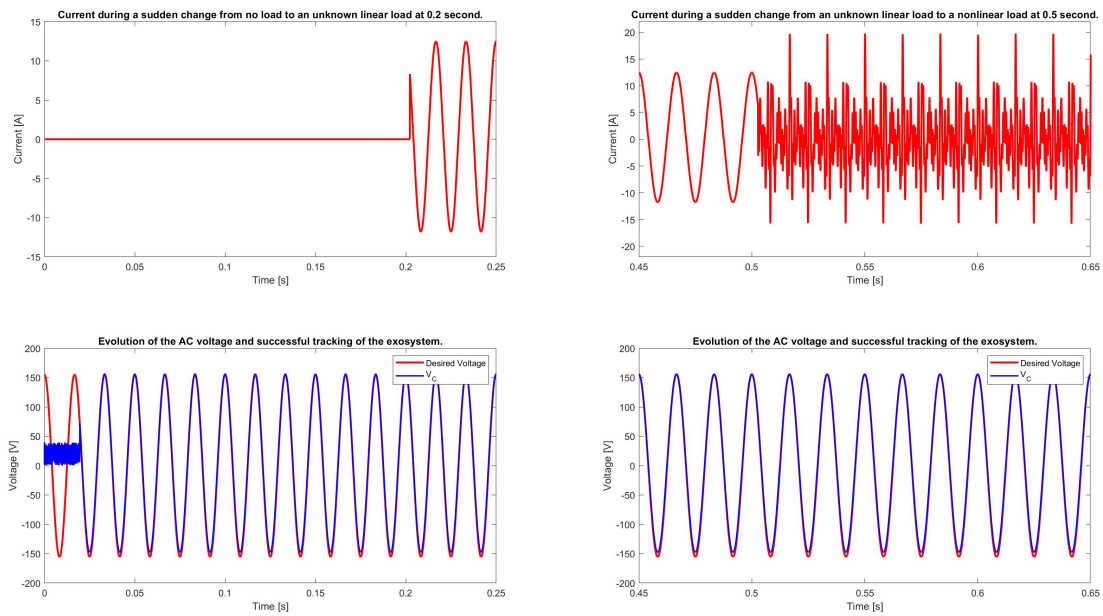

FIGURE 3 The behavior of the current at the load and the appropriate voltage tracking after using our observer-based event-triggered learning framework.

Theorem 4. Suppose that the triggering condition (36) and the concluding statement of Theorem 3 hold. Then the inter-event time T_j, $\forall j \in \mathbb{N}$ is strictly positive and has a positive lower bound.

Proof. According to the condition (36), we can write,

$$R_s(L_D \|e\|) \leq (1-\beta^2)\underline{\lambda}(\tilde{Q}) \left\|\hat{x}_{\text{aug}}\right\|^2 + R_s(\hat{W}_u^{\mathrm{T}}\phi_u(\bar{x}_{\text{aug}}))$$

with the first term being written as,

$$R_s(L\|e\|) = 2\int_{u^*(\bar{x}_{\text{aug}})}^{u^*(\hat{x}_{\text{aug}})} (V_{\text{dc}}\tanh^{-1}(\frac{v}{V_{\text{dc}}}))^{\mathrm{T}} dv \leq V_{\text{dc}}^2\big(u^*(\hat{x}_{\text{aug}}) - u^*(\bar{x}_{\text{aug}})\big)^{\mathrm{T}}\big(u^*(\hat{x}_{\text{aug}}) - u^*(\bar{x}_{\text{aug}})\big) \leq V_{\text{dc}}^2 L_D^2 \|e\|^2.$$

When an event is triggered at time $t = r_{j+1}$ that the following inequality holds,

$$\frac{\|e(r_{j+1})\|}{\|\hat{x}_{\text{aug}}(r_{j+1})\|} \geq \mathcal{P},\ j \in \mathbb{N}, \tag{40}$$

where $\mathcal{P} := \sqrt{\frac{(1-\beta^2)\underline{\lambda}\left(\tilde{Q}\right)}{V_{\text{dc}}^2 L_D^2}}$. Since we have that $e(r_j) = 0$, then the time that $\frac{\|e(t)\|}{\|\hat{x}_{\text{aug}}(t)\|}$ evolves from 0 to $\mathcal{P}$ provides a lower bound on the inter-event time. Now let us look at the dynamics of $\frac{\|e(t)\|}{\|\hat{x}_{\text{aug}}(t)\|}$. First, note that the evolution of the state satisfies the following,

$$\|\dot{\hat{x}}_{\text{aug}}\| \leq (W_{1\max}\Phi_M + \epsilon_{1\max})\|\hat{x}_{\text{aug}}\| + (W_{2\max}\Phi_M + \epsilon_{2\max})\|\hat{W}_u\|\|\bar{x}_{\text{aug}}\| + K_M\|\hat{W}_d\|\|\hat{x}_{\text{aug}}\| \leq \mathcal{L}(\|\hat{x}_{\text{aug}}\| + \|e\|)$$

where K is upper bounded by $K_M \in \mathbb{R}^+$, and $\mathcal{L} := ((W_{1\max}\Phi_M + \epsilon_{1\max}) + (W_{2\max}\Phi_M + \epsilon_{2\max})\|\hat{W}_u\| + K_M\|\hat{W}_d\|)$ is bounded since we have shown in Theorem 3 that $\|\hat{W}_u\|$ and $\|\hat{W}_d\|$ are bounded. Then we can bound the dynamics of $\frac{\|e(t)\|}{\|\hat{x}_{\text{aug}}(t)\|}$ as,

$$\frac{d}{dt}\frac{\|e(t)\|}{\|\hat{x}_{\text{aug}}(t)\|} \leq \mathcal{L}\left(1 + \frac{\|e(t)\|}{\|\hat{x}_{\text{aug}}(t)\|}\right)^2,\ \forall t \in (r_j, r_{j+1}],\ j \in \mathbb{N}.$$

After using the comparison Lemma (see Lemma 3.4 in[19]) we have the following result,

$$\frac{\|e(t)\|}{\|\hat{x}_{\text{aug}}(t)\|} \leq \frac{(t - r_j)\mathcal{L}}{1 - (t - r_j)\mathcal{L}},\ \forall t \in (r_j, r_{j+1}],\ j \in \mathbb{N}. \tag{41}$$

Computing (41) at time $t = r_{j+1}$ and combining with (40) yields,

$$\mathcal{P} \leq \frac{\|e(r_{j+1})\|}{\|\hat{x}_{\text{aug}}(r_{j+1})\|} \leq \frac{\mathcal{T}_j\mathcal{L}}{1 - \mathcal{T}_j}, \tag{42}$$

where $\mathcal{T}_j := (t - r_j)$.

Finally solving (42) for $\mathcal{T}_j$ results in,

$$\mathcal{T}_j \geq \frac{\mathcal{P}}{\mathcal{L}(1 + \mathcal{P})}.$$

Hence, there exists a positive lower-bound, which is a constant, for the next inter-event interval. The term $\frac{\|\bar{x}_{\text{aug}}(r_{j+1}) - \hat{x}_{\text{aug}}(r_{j+1})\|}{\|\hat{x}_{\text{aug}}(r_{j+1})\|}$ is continuous due to the fact that $\hat{x}_{\text{aug}}(r_{j+1})$ is never zero sine the closed-loop system has an asymptotically stable equilibrium point and never reaches zero in finite time. Therefore the absence of the Zeno behavior is proved. □

6 | SIMULATION

Consider the configuration of the off-grid VSI as shown in Figure 1 with $L = 1.1mH$, $C_{\text{ap}} = 50\mu F$, $R = 0.2\Omega$ and disturbance matrix given as $K = \begin{bmatrix}1\\0\end{bmatrix}$. The user defined matrices are defined as $Q = \begin{bmatrix}0.1 & 0\\0 & 0.2\end{bmatrix}$ to penalize appropriately the current and the voltage, $Q_r = I_2$, and $\tilde{Q}$ is picked according to (6) and $\gamma = 5$ to have a reasonable attenuation level with a worst-case disturbance given of the form (22). Note that (22) is not the actual disturbance of the system but the approximaton of the worst-case one that is used by the controller for attenuation. The actual disturbance can be anything as long as it satisfies (19). The control input is $\pm V_{\text{dc}}$ with $V_{\text{dc}} = 170$, the observer gain is $L_O = \begin{bmatrix}500 & 800\end{bmatrix}$, the observer weight parameters are given as $B_1 = \begin{bmatrix}6\times10^5 & 0\\0 & 6\times10^5\end{bmatrix}$, $B_2 = \begin{bmatrix}5\times10^4 & 0\\0 & 6\times10^4\end{bmatrix}$, $\alpha_1 = \alpha_2 = 2\times10^{-4}$, the tuning gain for the critic approximator is picked sufficiently larger than the actor ones, i.e., $\alpha_c = 30$, $\alpha_u = 1$ and $\alpha_d = 1$. The parameter β in (36) is picked as $\beta = 0.5$, such that the performance and the controller bandwidth are "balanced," and the Lipschitz constant is picked as $L_D = 3$.

For the load we will consider sudden changes. Hence for $0 \leq t < 0.263$ second we will not connect a load, from $0.263 \leq t < 0.5$ second we will connect a linear load and then at $t = 0.5$ second we will add a nonlinear load corresponding to a fluorescent lamp[5]. Figure 3 shows the evolution of the current at the load, and the output voltage waveform while the load is changing and $R - L - C$ have changed slightly as $L = 1.5mH$, $C_{\text{ap}} = 70\mu F$, and $R = 0.4\Omega$. Figure 4 shows the input DC voltage given as ±170. In order to check the efficiency we will compute the Total Harmonic Distortion (THD) (in relation to the fundamental frequency of the power grid source) of the output voltage and this is found to be THD= 1.48% which is well below the IEEE

Standards 519 − 1992 (a standard developed for utility companies and their customers in order to limit harmonic content and provide all users with better power quality) voltage distortion limits. The very small THD shows that our algorithm is robust to load and parameter changes, and disturbances. Figure 6 shows the inter-event times $T := r_j - r_{j-1}$

Figure 5 shows the evolution of the gap and the threshold for the first 0.2 second. A bandwidth improvement of almost 84.1% is achieved, while attenuating disturbances.

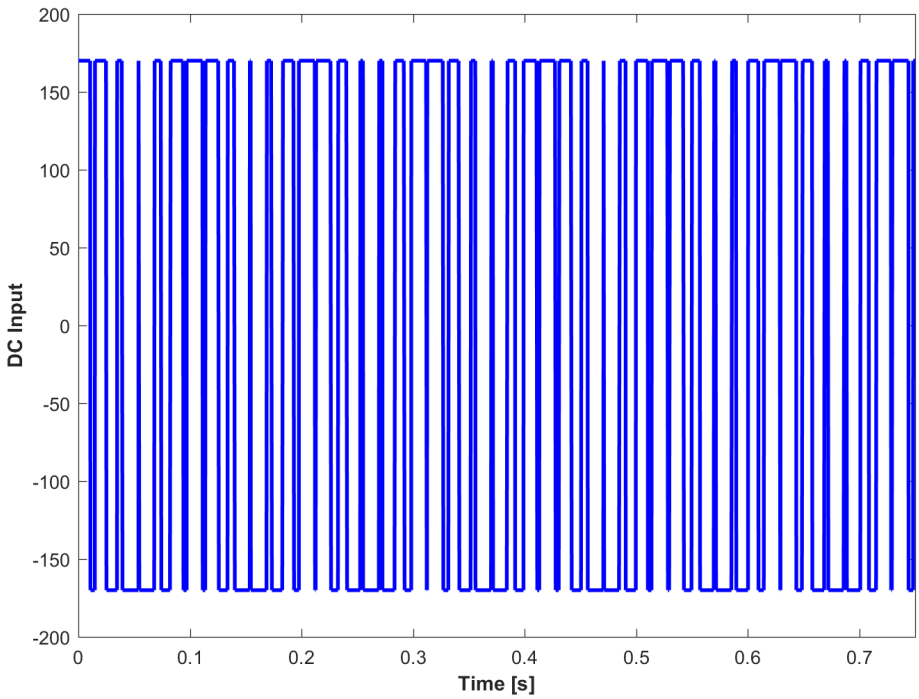

FIGURE 4 Evolution of the DC control input.

7 | CONCLUSIONS AND FUTURE WORK

We developed an observer-based optimal adaptive event-triggered control algorithm for a completely unknown off-grid VSI in order to attenuate the disturbance at the current and produce the desired AC behavior. Since the dynamics are not known, we use an adaptive observer to reconstruct the states based only at the output voltage. The control mechanism is constructed based on an impulsive actor/critic framework that approximates the optimal cost, the event-triggered optimal controller and the worst case disturbance. Rigorous stability proofs and simulation results are presented to show the efficacy of the developed approach. By incorporating saturated input voltages in the performance index, we avoid the need of pure pulse-width modulation control methods and phasor domain analysis. Thus, we do not require phasor domain analysis and the need to control the transients much faster than the fundamental period. The achieved THD of our framework is well below the IEEE Standards 519 − 1992 voltage distortion limits.

Future work will be concentrated on testing the present algorithm in hardware and extending the results to three-phase and parallel VSIs with delays.

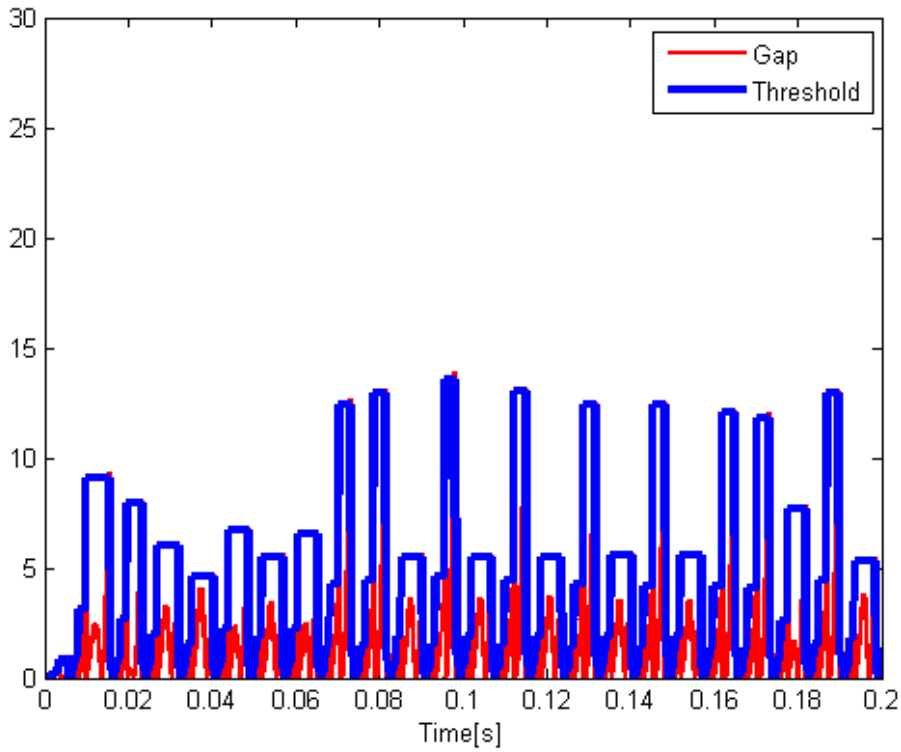

FIGURE 5 Evolution of the threshold, and the gap for the first 0.2 second.

APPENDIX

Proof of Theorem 2

The orbital derivative of V along the solution of (11), and (21)-(22) is given by,

$$\dot{V} = \frac{\partial V}{\partial \hat{x}_{\text{aug}}}^{\text{T}} \left(\tilde{f}(\hat{x}_{\text{aug}}) + \tilde{g}u(\bar{x}_{\text{aug}}) + \begin{bmatrix} K \\ \mathbf{0}_2 \end{bmatrix} d(\hat{x}_{\text{aug}}) \right) \tag{43}$$

and by solving the time triggered HJI (20) for $\frac{\partial V(\hat{x}_{\text{aug}})}{\partial \hat{x}_{\text{aug}}}^{\text{T}} \tilde{f}(\hat{x}_{\text{aug}})$ one obtains,

$$\begin{aligned} \frac{\partial V(\hat{x}_{\text{aug}})}{\partial \hat{x}_{\text{aug}}}^{\text{T}} \tilde{f}(\hat{x}_{\text{aug}}) &= \frac{\partial V}{\partial \hat{x}_{\text{aug}}}^{\text{T}} \left(\tilde{g}u(\hat{x}_{\text{aug}}) + \begin{bmatrix} K \\ \mathbf{0}_2 \end{bmatrix} d(\hat{x}_{\text{aug}}) \right) + \frac{1}{4\gamma^2} \frac{\partial V(\hat{x}_{\text{aug}})}{\partial \hat{x}_{\text{aug}}}^{\text{T}} \begin{bmatrix} KK^{\text{T}} & \mathbf{0}_{2\times 2} \\ \mathbf{0}_{2\times 2} & 0_{2\times 2} \end{bmatrix} \frac{\partial V(\hat{x}_{\text{aug}})}{\partial \hat{x}_{\text{aug}}} \\ &- R_s(-\theta\{\frac{1}{2}\tilde{g}^{\text{T}} \frac{\partial V(\hat{x}_{\text{aug}})}{\partial \hat{x}_{\text{aug}}}\}) - \hat{x}_{\text{aug}}^{\text{T}} \tilde{Q} \hat{x}_{\text{aug}}. \end{aligned} \tag{44}$$

By substituting (44) into (43) and after noting that $\frac{\partial V(\hat{x}_{\text{aug}})}{\partial \hat{x}_{\text{aug}}}^{\text{T}} \tilde{g} = -2\theta^{-T}(u(\hat{x}_{\text{aug}}))$ we have,

$$\dot{V} = \frac{1}{4\gamma^2} \frac{\partial V(\hat{x}_{\text{aug}})}{\partial \hat{x}_{\text{aug}}}^{\text{T}} \begin{bmatrix} KK^{\text{T}} & \mathbf{0}_{2\times 2} \\ \mathbf{0}_{2\times 2} & \mathbf{0}_{2\times 2} \end{bmatrix} \frac{\partial V(\hat{x}_{\text{aug}})}{\partial \hat{x}_{\text{aug}}} - R_s(u(\hat{x}_{\text{aug}})) - \hat{x}_{\text{aug}}^{\text{T}} \tilde{Q} \hat{x}_{\text{aug}} - 2\theta^{-T}(u(\hat{x}_{\text{aug}}))\big(u(\bar{x}_{\text{aug}}) - u(\hat{x}_{\text{aug}})\big). \tag{45}$$

By using the Assumption 1, we can write, $-R_s(u(\hat{x}_{\text{aug}})) - 2\theta^{-T}(u(\hat{x}_{\text{aug}}))\big(u(\bar{x}_{\text{aug}}) - u(\hat{x}_{\text{aug}})\big) \leq R_s(L_D \|e\|) - R_s(u(\bar{x}_{\text{aug}}))$ and hence (45) can be upper bounded as, $\dot{V} \leq -\beta^2 \underline{\lambda}(\tilde{Q}) \left\|\hat{x}_{\text{aug}}\right\|^2 + \frac{1}{4\gamma^2} \frac{\partial V(\hat{x}_{\text{aug}})}{\partial \hat{x}_{\text{aug}}}^{\text{T}} \begin{bmatrix} KK^{\text{T}} & \mathbf{0}_{2\times 2} \\ \mathbf{0}_{2\times 2} & \mathbf{0}_{2\times 2} \end{bmatrix} \frac{\partial V(\hat{x}_{\text{aug}})}{\partial \hat{x}_{\text{aug}}} + \Big(-(1-\beta^2)\underline{\lambda}(\tilde{Q}) \left\|\hat{x}_{\text{aug}}\right\|^2 + R_s(L_D \|e\|) - R_s(u(\bar{x}_{\text{aug}}))\Big)$.

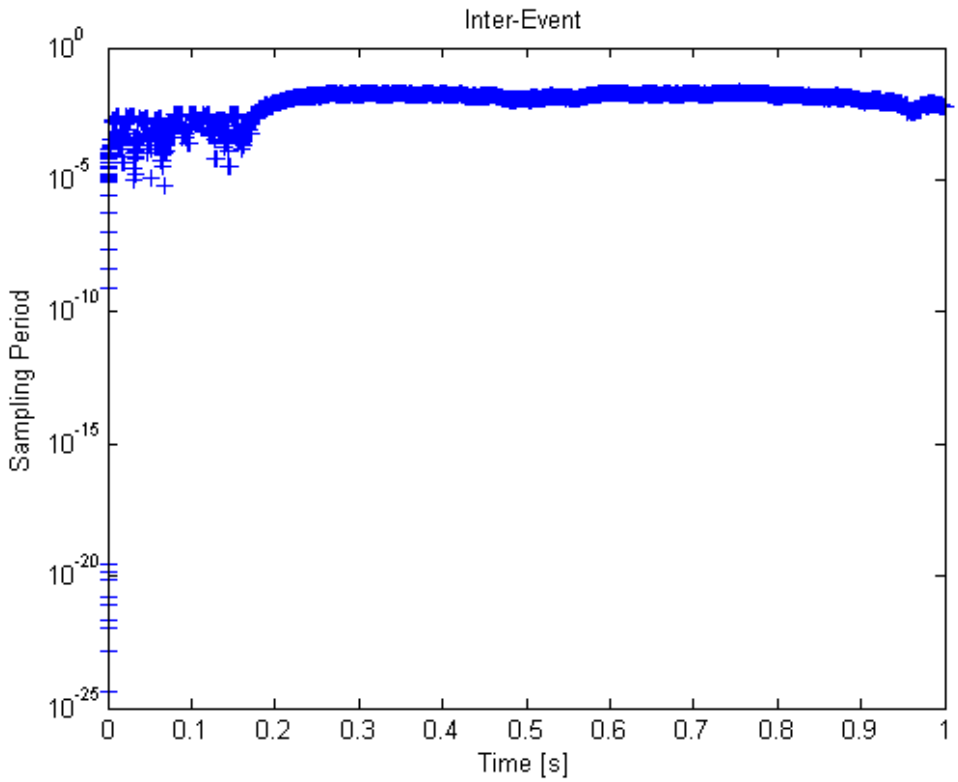

FIGURE 6 Inter-event as a function of time.

Finally, the closed-loop system is asymptotically stable given that (23) is satisfied for all $t \geq 0$. Now, since the function V is smooth, zero at zero, and converge to zero as $t \to \infty$ and by setting $V \equiv V^*$ as the optimal cost we can rewrite (5), using the event-triggered control updates

$$J(\cdot; u, d) = \int_0^\infty \left(R_s(u(\bar{x}_{\text{aug}})) - \gamma^2 \left\| d(\hat{x}_{\text{aug}}) \right\|^2 + \hat{x}_{\text{aug}}^{\text{T}} \tilde{Q} \hat{x}_{\text{aug}} \right) \mathrm{d}t + V^*(\hat{x}_{\text{aug}}(0)) + \int_0^\infty \frac{\partial V^*(\hat{x}_{\text{aug}})}{\partial \hat{x}_{\text{aug}}}^{\text{T}} \Bigg(\tilde{f}(\hat{x}_{\text{aug}}) + \tilde{g} u(\bar{x}_{\text{aug}}) + \begin{bmatrix} K \\ \mathbf{0}_2 \end{bmatrix} d(\hat{x}_{\text{aug}}) \Bigg) \mathrm{d}t, \tag{46}$$

subtracting zero from (46) by using the equation (19) and completing the squares yields,

$$J(\cdot; u, d) = \int_0^\infty \left(R_s(u(\bar{x}_{\text{aug}}) - u^*(\bar{x}_{\text{aug}})) - \gamma^2 \left\| d(\hat{x}_{\text{aug}}) - d^*(\hat{x}_{\text{aug}}) \right\|^2 \right) \mathrm{d}t + V^*(\hat{x}_{\text{aug}}(0)) + \int_0^\infty R_s\left(u^*(\hat{x}_{\text{aug}}) - u^*(\bar{x}_{\text{aug}}) \right). \tag{47}$$

Setting $u(\bar{x}_{\text{aug}}) = u^*(\bar{x}_{\text{aug}})$ in (47), leads to,

$$J(\cdot; u^*, d) = \int_0^\infty \left(-\gamma^2 \left\| d(\hat{x}_{\text{aug}}) - d^*(\hat{x}_{\text{aug}}) \right\|^2 \right) \mathrm{d}t + V^*(\hat{x}_{\text{aug}}(0)) + \int_0^\infty R_s\left(u^*(\hat{x}_{\text{aug}}) - u^*(\bar{x}_{\text{aug}}) \right) \mathrm{d}t,$$

setting $d(\hat{x}_{\text{aug}}) = d^*(\hat{x}_{\text{aug}})$ in (47) leads to, $J(\cdot; u, d^*) = \int_0^\infty \left(R_s(u(\bar{x}_{\text{aug}}) - u^*(\bar{x}_{\text{aug}})) \right) \mathrm{d}t + V^*(\hat{x}_{\text{aug}}(0)) + \int_0^\infty R_s\left(u^*(\hat{x}_{\text{aug}}) - u^*(\bar{x}_{\text{aug}}) \right) \mathrm{d}t$, and finally setting $u(\bar{x}_{\text{aug}}) = u^*(\bar{x}_{\text{aug}})$ and $d(\hat{x}_{\text{aug}}) = d^*(\hat{x}_{\text{aug}})$ in (47) yields,

$$J^*(\cdot; u^*, d^*) = V^*(\hat{x}_{\text{aug}}(0)) + \int_0^\infty R_s\left(u^*(\hat{x}_{\text{aug}}) - u^*(\bar{x}_{\text{aug}}) \right) \mathrm{d}t.$$

Thus, condition (7) follows.

Proof of Theorem 3

In order to prove stability we have to combine the continuous and the discrete time dynamics under the framework of impulsive systems, inspired by the work of[11,13]. Hence, the time derivative of $\psi := \begin{bmatrix}\hat{x}_{\text{aug}}^{\text{T}} & \bar{x}_{\text{aug}}^{\text{T}} & \tilde{W}_c^{\text{T}} & \tilde{W}_u^{\text{T}} & \tilde{W}_d^{\text{T}}\end{bmatrix}^{\text{T}}$ for $t \in (r_j, r_{j+1}],\ j \in \mathbb{N}$ can be written as,

$$\dot{\psi} = \begin{bmatrix} \tilde{f} + \tilde{g}\left(W_u^* - \tilde{W}_u\right)^{\text{T}}\phi_u + \begin{bmatrix} K \\ \mathbf{0}_2 \end{bmatrix}\left(W_d^* - \tilde{W}_d\right)^{\text{T}}\phi_d \\ 0 \\ -\alpha_c \frac{\Delta\phi\Delta\phi^{\text{T}}}{(\|\Delta\phi\|^2+1)^2}\tilde{W}_c + \alpha_c \frac{\Delta\phi}{(\|\Delta\phi\|^2+1)^2}\epsilon_{\tilde{W}_c} \\ 0 \\ \Lambda \end{bmatrix}$$

where $\Lambda = -\alpha_d \phi_u(\hat{x}_{\text{aug}})\left(\tilde{W}_d^{\text{T}}\phi_d(\hat{x}_{\text{aug}}) + \epsilon_d^{\text{T}}\phi_d(\hat{x}_{\text{aug}}) - \frac{1}{2\gamma^2}\begin{bmatrix} K \\ \mathbf{0}_2 \end{bmatrix}^{\text{T}} \frac{\partial \phi_c}{\partial \hat{x}_{\text{aug}}}\tilde{W}_c - \frac{1}{2}\begin{bmatrix} K \\ \mathbf{0}_2 \end{bmatrix}^{\text{T}} \frac{\partial \epsilon_c}{\partial \hat{x}_{\text{aug}}}\right)^{\text{T}}$ and the jump dynamics for $t = r_j, j \in \mathbb{N}$, are given by, $\psi^+ = \psi(t) + \begin{bmatrix} 0 \\ e(t) \\ 0 \\ 0 \\ \Gamma_j \end{bmatrix}$, $t = r_j,\ j \in \mathbb{N}$, where $\Gamma_j = \tilde{W}_u(t) - \alpha_u \phi_u(\hat{x}_{\text{aug}}(t))\Big(\tilde{W}_u^{\text{T}}\phi_u(\hat{x}_{\text{aug}}(t)) + \epsilon_u^{\text{T}}\phi_u(\hat{x}_{\text{aug}}(t)) + \theta\{\frac{1}{2}\tilde{g}(\hat{x}_{\text{aug}}(t))^{\text{T}}\frac{\partial \phi_u}{\partial \hat{x}_{\text{aug}}}\tilde{W}_c + \theta\{\frac{1}{2}\tilde{g}(\hat{x}_{\text{aug}}(t))^{\text{T}}\frac{\partial \epsilon_c}{\partial \hat{x}_{\text{aug}}}\}\Big)^{\text{T}}$.

We shall consider the continuous and jump dynamics separately. First, in order to prove stability for the continuous part we will start with the following Lyapunov function $\mathcal{V} : \mathbb{R}^2 \times \mathbb{R}^2 \times \mathbb{R}^{h_1} \times \mathbb{R}^{h_2} \times \mathbb{R}^{h_3} \to \mathbb{R}$,

$$\mathcal{V}(\psi) = V^*(\hat{x}_{\text{aug}}) + V^*(\bar{x}_{\text{aug}}) + \frac{1}{2}\left\|\tilde{W}_c\right\|^2 + \frac{1}{2\alpha_u}\left\|\tilde{W}_u\right\|^2 + \frac{1}{2\alpha_d}\left\|\tilde{W}_d\right\|^2. \tag{48}$$

Now after taking the time derivative of (48) and by noting that $\frac{\mathrm{d}V^*(\bar{x}_{\text{aug}})}{\mathrm{d}t} = 0$ and $\frac{\mathrm{d}}{\mathrm{d}t}\frac{1}{2\alpha_u}\left\|\tilde{W}_u\right\|^2 = 0$ we have between the jumps,

$$\dot{\mathcal{V}} = \frac{\partial V^*(\hat{x}_{\text{aug}})}{\partial \hat{x}_{\text{aug}}}\dot{\hat{x}}_{\text{aug}} + \tilde{W}_c^{\text{T}}\dot{\tilde{W}}_c + \frac{1}{\alpha_d}\tilde{W}_d^{\text{T}}\dot{\tilde{W}}_d, \tag{49}$$

which after substituting (11), (34), (35) in (49), grouping the similar terms together and using the condition (36) yields,

$$\dot{\mathcal{V}} \le -\beta^2\underline{\lambda}(Q)\left\|\hat{x}_{\text{aug}}\right\|^2 - \left(\alpha_c\underline{\lambda}\left(\frac{\Delta\phi\Delta\phi^{\text{T}}}{(\|\Delta\phi\|^2+1)^2}\right) - \frac{1}{2\alpha_c} - \frac{\phi_{\text{cdmax}}^2}{4\gamma^2}\right)\left\|\tilde{W}_c\right\|^2 - \left(\phi_{\text{dmax}}^2 - \frac{3}{4} - \frac{\phi_{\text{dmax}}^2}{4\gamma^2}\right)\left\|\tilde{W}_d\right\|^2 + \mu_d, \tag{50}$$

where $\mu_d = \frac{1}{4\alpha_c}\epsilon_{\tilde{W}_c} + \frac{1}{4}\left(2\phi_{\text{dmax}}^4\epsilon_{\text{dmax}}^2 + \phi_{\text{dmax}}^2\epsilon_{\text{cdmax}}^2\right)$. Given the inequalities, (37)-(38), there exists a class-$\mathcal{K}$ function k_1 to write (50) as

$$\dot{\mathcal{V}} \le -k_1\left(\|\psi\|\right) + \mu_d, \tag{51}$$

from which we can conclude that $\dot{\mathcal{V}} < 0$ whenever the state ψ lies outside the set $\Omega_\psi = \{\psi : k_1\left(\|\psi\|\right) \le \mu_d\}$ from which UUB of the continuous closed-loop signals follows.

For the jump dynamics, for $t = r_j, j \in \mathbb{N}$, we will consider the following difference Lyapunov function, $\Delta\mathcal{V}(\psi) = V^*(\hat{x}_{\text{aug}}^+) - V^*(\hat{x}_{\text{aug}}(t)) + V^*(\bar{x}_{\text{aug}}^+) - V^*(\bar{x}_{\text{aug}}(t)) + V_c(\tilde{W}_c^+) - V_c(\tilde{W}_c(t)) + V_d(\tilde{W}_d^+) - V_d(\tilde{W}_d(t)) + \frac{1}{2\alpha_u}\left\|\tilde{W}_u^+\right\|^2 - \frac{1}{2\alpha_u}\left\|\tilde{W}_u(t)\right\|^2$ where $V_c = \frac{1}{2}\left\|\tilde{W}_c\right\|^2$, $V_d = \frac{1}{2\alpha_d}\left\|\tilde{W}_d\right\|^2$ and from the continuous-time dynamics we have that $V^*(\hat{x}_{\text{aug}}^+) \le V^*(\hat{x}_{\text{aug}}(t))$, $V_c(\tilde{W}_c^+) \le V_c(\tilde{W}_c(t))$, and $V_d(\tilde{W}_d^+) \le V_d(\tilde{W}_d(t))$ for $t = r_j, j \in \mathbb{N}$. Now since the states $\hat{x}_{\text{aug}}$ are UUB from (51) then since $\bar{x}_{\text{aug}} = \hat{x}_{\text{aug}}(t)$ for $t = r_j, j \in \mathbb{N}$ it is true that $V^*(\bar{x}_{\text{aug}}^+) \le V^*(\bar{x}_{\text{aug}})$ which can lead us to write $\Delta\mathcal{V}(\bar{x}_{\text{aug}}) \le -k_2\left(\left\|\bar{x}_{\text{aug}}\right\|\right)$ with k_2 a class-$\mathcal{K}$ function. After some algebra in the error actor jump dynamics (similarly to the disturbance weight error in the continuous dynamics) we can write the Lyapunov difference as, $\Delta\mathcal{V}(\psi) \le -\left(\phi_{\text{umax}}^2 - \frac{\alpha_u}{2}\phi_{\text{umax}}^2\right)\left\|\tilde{W}_u^+\right\|^2 + \mu_u$ where $\mu_u = 2\phi_{\text{umax}}V_{\text{dc}} + \frac{1}{2}\phi_{\text{umax}}^4\epsilon_{\text{umax}}^2$. Finally, using the result from (39), we can conclude that the jump dynamics are UUB as long as ψ lies outside the set $\Omega_{\Delta\psi} = \{\psi : k_2\left(\|\psi\|\right) \le \mu_u\}$.

References

1. B. D. O Anderson, and J. B. Moore, *Linear Optimal Control*, Englewood Cliffs, Prentice Hall, NJ, 1971
2. T. Basar, G. J. Olsder, *Dynamic noncooperative game theory* (2nd ed.), Philadelphia, PA: SIAM, 1999
3. D. P. Borgers, W. P. M. H. Heemels, "Event-separation properties of event-triggered control systems," *Automatic Control, IEEE Transactions*, vol. 59, no. 10, pp. 2644-2656, 2014
4. S.R. Bull, "Renewable energy today and tomorrow," *Proceedings of the IEEE*, vol. 89, no. 8, pp. 1216-1226, 2001
5. M. Cervi, A. R. Seidel, F. E. Bisogno, and D. Prado, "Fluorescent Lamp Model based on the Equivalent Resistance Variation," *Proc. IEEE Intl. Conf. on Ind. Appl.*, pp. 680-684, 2002
6. Y. Del Valle, G.K. Venayagamoorthy, S. Mohagheghi, J.-C. Hernandez, and R.G. Harley, "Particle swarm optimization: Basic concepts, variants and applications in power systems," *IEEE Transactions on Evolutionary Computation*, vol. 12, no. 2, pp. 171-195, 2008
7. V. S. Dolk, D. P. Borgers, and W. P. M. H. Heemels. "Output-Based and Decentralized Dynamic Event-Triggered Control With Guaranteed $\mathcal{L}_p$-Gain Performance and Zeno-Freeness," *IEEE Transactions on Automatic Control*, vol. 62, no. 1, pp. 34-49, 2017
8. S. Eren, M. Pahlevaninezhad, A. Bakhshai, and P.K. Jain, "Composite nonlinear feedback control and stability analysis of a grid-connected voltage source inverter with LCL filter," *IEEE Transactions on Industrial Electronics*, vol. 60, no. 11, pp. 5059-5074, 2013
9. D. Ernst, M. Glavic, and L. Wehenkel, "Power systems stability control: reinforcement learning framework," *IEEE Transactions on Power Systems*, vol. 19, no. 1, pp. 427-435, 2004
10. A. Girard, "Dynamic triggering mechanisms for event-triggered control," *Automatic Control, IEEE Transactions on*, vol. 60, no. 7, pp. 1992-1997, 2015
11. W. M. Haddad, V. Chellaboina, and S. G. Nersesov, *Impulsive and Hybrid Dynamical Systems: Stability, Dissipativity, and Control*, Princeton, NJ: Princeton University Press, 2006
12. W.P.M.H. Heemels, M.C.F. Donkers, and A.R. Teel, "Periodic event triggered control for linear systems," *IEEE Transactions on Automatic Control*, vol. 58, no. 4, pp. 847-861, 2013
13. J. P. Hespanha, D. Liberzon, and A. R. Teel, "Lyapunov conditions for input-to-state stability of impulsive systems," *Automatica*, vol. 44, no. 11, pp. 2735-2744, 2008
14. K. Hornik, M. Stinchcombe, and H. White, "Universal approximation of an unknown mapping and its derivatives using multilayer feedforward networks," *Neural Networks*, vol. 3, no. 5, pp. 551-560, 1990
15. S.N. Huang, K.K. Tan, and T.H. Lee, "Further result on a dynamic recurrent neural-network-based adaptive observer for a class of nonlinear systems," *Automatica*, vol. 41, no. 12, pp. 2161-2162, 2005
16. P. A. Ioannou, and B. Fidan, *Adaptive Control Tutorial*, Advances in design and control, SIAM (PA), 2006
17. D. Kalyanraj, and S.L. Prakash, "Design and performance analysis of different current control strategies of voltage source inverter," *International Conference on Power, Energy and Control (ICPEC)*, pp. 310-315, 2013
18. Y. H. Kim, F. L. Lewis, and C. T. Abdallah, "A dynamic recurrent neural-network-based adaptive observer for a class of nonlinear systems," *Automatica*, vol. 33, no. 8, pp. 1539-1543, 1997
19. H. K. Khalil, *Nonlinear Systems*, Prentice Hall, 2002
20. M. Lemmon, "Event-Triggered Feedback in Control, Estimation, and Optimization," In: Bemporad A., Heemels M., Johansson M. (eds) Networked Control Systems, Lecture Notes in Control and Information Sciences, vol 406. Springer, London, 2010

21. F.L. Lewis, D. Vrabie, and K.G. Vamvoudakis, "Reinforcement learning and feedback control: Using natural decision methods to design optimal adaptive controllers," *IEEE Control Systems*, vol. 32, no. 6, pp. 76-105, 2012

22. T. Liu, and Z-P Jiang, "Event-based control of nonlinear systems with partial state and output feedback," *Automatica*, vol. 53, pp. 10-22, 2015

23. M. Mazo, M. Cao, "Asynchronous decentralized event-triggered control," *Automatica*, vol. 50, no. 12, pp. 3197-3203, 2014

24. S. Mohagheghi, Y. Del Valle, G.K. Venayagamoorthy, and R.G. Harley, "A proportional-integrator type adaptive critic design-based neurocontroller for a static compensator in a multimachine power system," *IEEE Transactions on Industrial Electronics*, vol. 54, no. 1, pp. 86-96, 2007

25. M. Pahlevaninezhad, P. Das, J. Drobnik, G. Moschopoulos, P.K. Jain, and A. Bakhshai, "A nonlinear optimal control approach based on the control-lyapunov function for an ac/dc converter used in electric vehicles," *IEEE Transactions on Industrial Informatics*, vol. 8, no. 3, pp. 596-614, 2012

26. P. Tabuada, "Event-Triggered Real-Time Scheduling of Stabilizing Control Tasks", *IEEE Trans. on Automatic Control*, vol. 52, no. 9. pp. 1680-1685, 2007

27. P. Tallapragada and N. Chopra, "On event triggered tracking for nonlinear systems," *IEEE Transactions on Automatic Control*, vol. 58, no. 9, pp. 2343-2348, 2013

28. K. G. Vamvoudakis, and J. P. Hespanha "Online optimal switching of single phase dc/ac inverters using partial information," to appear in *American Control Conference*, 2014.

29. K. G. Vamvoudakis, and J. P. Hespanha, "Online Optimal Operation of Parallel Voltage Source Inverters using Partial Information," *IEEE Transactions on Industrial Electronics*, vol. 64, no. 5, pp. 4296-4305, 2017.

30. A. J. Van der Schaft, "L_2-gain analysis of nonlinear systems and nonlinear state feedback H_∞ control," *IEEE Transactions on Automatic Control*, vol. 37, no. 6, pp. 770-784, 1992

31. G.K. Venayagamoorthy, "Dynamic, stochastic, computational, and scalable technologies for smart grids," *IEEE Computational Intelligence Magazine*, vol. 6, no. 3, pp. 22-35, 2011

32. D. Vrabie, K. G. Vamvoudakis, and F. L. Lewis, *Optimal Adaptive Control and Differential Games by Reinforcement Learning Principles*, Control Engineering Series, IET Press, 2012

How to cite this article: K. G. Vamvoudakis, F R. Pour Safaei, and J. P. Hespanha (2018), Robust Event-Triggered Output Feedback Learning Algorithm for Voltage Source Inverters with Unknown Load and Parameter Variations, *International Journal of Robust and Nonlinear Control*, *2018;00:1–6*.